Using molecular dynamic simulations to compare pH effects on the diphtheria toxin and its mutant (E349K)

Soheila Ghaderi[1], Mohammad Reza Bozorgmehr[2], Shirin Tarahomjoo[3]*, Majid Esmaelizad[4], Mojtaba Noofeli[5]

[1]Division of Central Laboratory, Department of Biotechnology, Razi Vaccine and Serum Research Institute, Agricultural Research, Education and Extension Organization (AREEO), Karaj 31975/148, Iran

[2]Department of Chemistry, Mashhad Branch, Islamic Azad University, Mashhad, Iran

[3]Division of Genomics and Genetic Engineering, Department of Biotechnology, Razi Vaccine and Serum Research Institute, Agricultural Research, Education and Extension Organization (AREEO), Karaj 31975/148, Iran.

[4]Division of Central Laboratory, Department of Biotechnology, Razi Vaccine and Serum Research Institute, Agricultural Research, Education and Extension Organization (AREEO), Karaj 31975/148, Iran

[5]Department of DTP Vaccine Production, Razi Vaccine and Serum Research Institute, Agricultural Research, Education and Extension Organization (AREEO), Karaj 31975/148, Iran

* *Corresponding:*

Email: starahomjoo@gmail.com

Tel: 98 026 34570038

Postal Code: 3197619751

Abstract

Mutagenesis of amino acid is a powerful tool to investigate the molecular structure and the protein function. The mutation of E349 of diphtheria toxin (DT) to K inhibits the molecular cytotoxicity in mammalian cells. In addition, protein conformations and structures are affected by pH. In this work, we therefore aim to investigate the effect of mutation on the structural stability and conformation of DT at different pH levels (acidic, neutral, basic) using molecular dynamics (MD) simulations. Our results indicated that fluctuations of amino acid residues in the catalytic domain(C) and the receptor-binding domain (R) of DT are more than those of the mutant protein (E349K) at all studied pHs. The secondary structure analysis showed that the β-sheet content of E349K was lower than that of DT. The radius of gyration (Rg) and the root mean square deviation (RMSD) of E349K were more than those of DT regardless of pH. The conformational stability and compactness of DT were more than those of E349K. In conclusion, MD simulations predicted the lack of the receptor binding and the catalytic activities of E349K at all pHs. These results can be used for stability studies in the produce recombinant vaccine based on bacteria toxins.

Keywords: Variable pH; Secondary structure; Targeted mutagens; Molecular dynamics simulations;

Introduction

The diphtheria toxin (DT) structure consists of 535 amino acids in two fragments, A and B, connected through a disulfide bond (Malito et al., 2012). It includes the catalytic (C) domain (amino acid residues 1-188), the transmembrane or translocation (T) domain (amino acid residues 201-378), and the receptor-binding (R) domain (amino acids 379-535). The disulfide bridge at

the amino acids C186–C201 connects C-terminus of the C domain to N-terminus of the T domain (Gill et al., 1972). Following endocytosis of the toxin, the translocation is induced by exposure of the surface-bound toxin to low pH (Papini et al., 1993). The fragment A is released in the cytosol and as a result of reducing the disulfide bond linking the fragments A and B at the acidic pH (Moskaug et al., 1988). Previous study suggested that the translocation of the fragment A across the membrane was initiated at the C terminus(Falnes and Olsnes, 1995). The fragment B is responsible for binding of the toxin to the cells, through heparin-binding epidermal growth factor (HBEG) precursor as the receptor(Uchida et al., 1972) (Naglich et al., 1992). Genetically modified toxoids and their fragments are currently regarded as more promising components for vaccines than the chemically modified analogues of the natural toxins, since they are cheaper, quite immunogenic, and cause fewer complications in multiple vaccinations(Robbins et al., 2005).

Some of the mutations that impair the toxin's lethality for *Escherichia coli* affect its membrane interactions and cytotoxicity in mammalian cells, such as what observed in E349K mutant (O'Keefe et al., 1992). The E349K mutation showed no cytotoxicity at the highest concentration tested and the low pH (pH4.4). Neither receptor-binding activity DT nor its ADP-ribosyltransferase activity was affected by the E349K mutation (O'Keefe et al., 1992).

Using Bioinformatics method and molecular dynamics simulations (MD), be targeted mutagens are an important tool in the theoretical study of biological molecules. This computational method calculates the time dependent behavior of a molecular system. MD simulations have provided detailed information on the fluctuations and conformational changes of proteins and nucleic acids. These methods are now routinely used to investigate the structure, dynamics and thermodynamics (van der Spoel et al., 2008).

In this work, we aim to compare the effects of the amino acid mutation and pH

on the structural stability of DT. Therefore, we analyzed the DT structure and its mutant (E349K) at different pH levels (3, 7, 10) using molecular dynamics simulations. The conformational changes were studied by comparison of secondary and tertiary structures. Furthermore, results were demonstrated using the root mean square fluctuation (RMSF), Radius of gyration (Rg) and Root mean square of deviation (RMSD). The results of this study are applicable to the design of DT vaccines with the appropriate structural stability.

Computational Details

The DT structure was retrieved from Protein Data Bank (PDB). The protein PDB ID of 1F0L was considered (Bennett et al., 1994). The three-dimensional structure of DT mutant (E349K) was prepared using the molecular graphics program PYMOL, which is a robust, stable and widely used program. The protonation fixing process was done with DT and its mutant (E349K) at different pH levels (3, 7, 10) by using H++ server, which was the input for molecular dynamics simulation(Hess et al., 2008). The molecular dynamics simulations were done by GROMACS 4.5.4 package by using AMBER99SB force field and periodic boundary conditions. Six simulation boxes were used separately with dimensions of 9.5 × 9.5 × 9.5 nm^3 (Satpathy et al., 2010). Then, the boxes were filled with the appropriate number of water molecules. In order to neutralize the system, the appropriate numbers of Na and Cl ions were added to each box. To eliminate any undesirable contact atoms and initial kinetic energy in the simulation boxes, the energy was minimized by applying the steepest descent algorithm. Then each of the defining systems was equilibrated in two stages, including 5 ns, NPT and NVT simulations at 300K and 1bar. The pressure and the temperature were controlled using Parrinello-Rahman barostat and V-rescale thermostat respectively(Bussi et al., 2007; Parrinello et al., 1983). For each component of the systems, PME algorithm was applied to estimate the electrostatic interactions(Darden et al., 1993) ..INCS and SETTLE algorithms

were used to fix the chemical bonds in atoms of proteins and solvent molecules respectively(Hess et al., 1997) (Miyamoto and Kollman, 1992). All of the simulations were run for 20ns, and the time step of 2fs. Secondary structures and tertiary structures of proteins were obtained using the Yasara view software (www.yasara.org). Tertiary structures were compared with CM view software version 1.1.1(Vehlow et al., 2011). All simulations were repeated to test the convergence of the results.

Results and Discussion

Following molecular dynamic simulations, we studied fluctuations of the key amino acid residues in DT and its mutant (E349K). For this purpose, we used RMSF, which is an indicator of the macromolecule flexibility. Highly flexible domains show high fluctuations in amino acid residues. Therefore, these domains tend to unfold and are unstable. The highly fluctuating residues are probably the initial points of the protein denaturation (Bozorgmehr and Housaindokht, 2008; Housaindokht and Monhemi, 2013). Our RMSF analysis revealed that the amino acid residues G64 and H520 of the DT structure showed considerable fluctuations at pH 10 (Fig. 1A). However, amino acids K39 and K349 were highly fluctuated in the E349K mutant at the same pH. Also, the RMSF chart at pH 3 (Fig. 1B) showed that fluctuations of residues G171, A185-A187 and K534 of the DT structure were notable, whereas residues K349, F410 and H520 showed high fluctuations in the mutant structure. These results of RMSF at neutral pH showed that residues fluctuation of DT in C domain and R domain are more than those at E349K (Fig. 1C).

Moreover, amino acid fluctuations in C and R domains of DT were more than in those of E349K at pH3. These results suggested that the structural flexibility of C and R domains of the DT for joining to their relevant cellular receptors was higher than that of C and R domains of the mutant. Previous studies of proteins at low frequency infrared modes also indicated that amino acid fluctuations upon

substrate binding involved the transition of the rigid protein structures to unfolded states (Honig et al., 1976).

Radius of gyration for a protein is a measure of its compactness. A larger Rg shows that the structure is less compact (Lobanov et al., 2008). The compactness has been defined as the ratio of accessible surface area of a protein to the surface area of the ideal sphere at the same volume (Tsai et al., 1997; Tsai and Nussinov, 1997). Rg values of DT and E349K structures were shown through the simulations at pH3, pH7 and pH10 (Fig. 2A, 2B and 2C, respectively). These results indicated that the structural compactness of the E349K mutant was lower than that of DT during the simulations at all pH levels.

Several studies simulated the folding of extended polypeptide chains and produced compact globular forms. As a measure of their success, RMSDs of the atomic positions in their models were calculated in relation to the native structures obtained by the crystallography. This deviation offered some measures for the relative effectiveness of the simulations for predicting the protein folding (Cohen and Sternberg, 1980; Kumar and Purohit, 2012). The RMSD is often calculated using only one atom per amino acid residue e. g. the α-carbon in order to evaluate the global conformational change in a protein. It is generally calculated after a least-squares fit to remove the effects of global transmission and rotation of a protein. Therefore, the differences between the two structures are minimized. Several efficient algorithms have been developed for calculations of RMSDs(Coutsias et al., 2004; McLachlan, 1982; Pitera, 2014). The plots of RMSD were obtained from molecular dynamics simulations. The overall RMSD was compared between DT and E349K at pH 3, pH7 and pH 10 (Fig. 3A, 2B and 2C). The overall RMSD values of DT and the mutant were 0.1559 nm and 0.1789 nm respectively at pH 3. Mutant lingered distinguished till the end and exhibited higher aberration. Also the overall RMSD for the mutant structure (0.1198 nm) was more than that for DT (0.1174 nm) at pH 10. The RMSD values

of the DT and mutant (E349K) structures were 0.12nm and 0.17nm respectively at neutral pH. The RMSD graphs of E349K were at higher levels compared with those of DT at all pHs.

The components of secondary structures of DT and E349K at pH3, pH7 and pH10 were determined using Yasara software (Table 1). The secondary structure of DT at pH 3 contained 28.8% β-Sheet. However, the β-Sheet content of the E349K structure was slightly lower than that of DT at the same pH. The β-Sheet content of DT was higher than that of the mutant at pH 10. The β-Sheet content of the mutant protein (E349K) decreased compared with that of DT at neutral pH.

In β-Sheets, strands of proteins lie adjacent to each other interacting laterally via hydrogen bonds between backbone carbonyl oxygen and amino group hydrogen atoms. Increasing the β-sheet contents of proteins enhanced the protein stability (Mowshowitz, 2010). Therefore, our results suggested that the stability of secondary structure of DT was similar to that of the mutant protein at pH 3. In contrast, the stability of secondary structure of DT was higher than that of the mutant protein at pH10 and pH7.

In order to evaluated tertiary structures of E349K and DT, the contact maps of the proteins were evaluated at pH3 and pH10 by version 1.1.1 of CM View (Vehlow et al., 2011). Our results showed remarkable differences in amino acids A185, C186, A187 at pH 3 and at amino acid residues R170-A177 at pH 10. All of these amino acids resided in coil contents of the proteins and were part of the C domain. However, no differences exist between the contacts of DT and E349K structures in the fragment B at both of the acidic and basic pHs. The disulfide bridge C186–C201 that connects C-terminus of the C domain to N-terminus of the T domain did not contain in the mutant (E349K) but observed in the wild of the diphtheria toxin (see Fig. 4A and Fig. 4B). This disulfide bridge is essential for toxin activity(Chenal et al., 2002).

Conclusions

Our results showed that the stability of the E349K structure decreased in comparison with that of the DT structure at different pHs. The disulfide bridge C186–C201 that connects C-terminus of the C domain to N-terminus of the T domain did not contain in the mutant (E349K), however presented in DT at neutral pH. These disulfide bridge essential is for the DT activity. In this work, we have found RMSF fluctuations of residues in catalytic and receptor binding domains of DT, including G1-C186 and K534 -S535, which more than those of its mutant (E349K) at all pHs. On the other hand, residue fluctuations, including K349 -V351 of E349K are more than those of DT, which does not have any role in the receptor binding domain and therefore loses its connection to sequential binding of substrates. Fluctuations of the amino acids in the DT were visible in the C and R domains at pH3. However, fluctuations in the E349K mutant decreased in these domains. Therefore, the tendency of E349K protein was lower than that of the DT for joining to the cellular receptors. As a result, E349K will not able to elicit appropriate immune responses and it is not suitable for preparation of recombinant vaccines. These results can be used for stability studies in the produce recombinant vaccine based on bacteria toxins.

This method can be used to evaluate conformational changes of toxins and proteins as well as vaccine candidates. Because demonstration detail atom of the structure in the toxins that is an important aspect for predicting of activities the receptor binding and the catalytic domains.

Conflict of interest disclosure

The authors declare no conflict of interest related to this work.

Acknowledgements

This work was financially supported by Razi Vaccine and Serum Research Institute under grant number (2-18-18-94116).

References

Bennett, M., Choe, S., Eisenberg, D., 1994. Refined structure of dimeric diphtheria toxin at 2.0 Å resolution. Protein Science 3, 1444-1463.
Bozorgmehr, M.R., Housaindokht, M.R., 2008. Effects of sodium dodecyl sulfate concentration on the structure of bovine carbonic anhydrase: molecular dynamics simulation approach. Romanian Journal of Biochemistry 47, 15.
Bussi, G., Donadio, D., Parrinello, M., 2007. Canonical sampling through velocity rescaling. The Journal of chemical physics 126, 014101.
Chenal, A., Nizard, P., Gillet, D., 2002. Structure and function of diphtheria toxin: from pathology to engineering. Toxin Reviews 21, 321-359.
Cohen, F.E., Sternberg, M.J., 1980. On the prediction of protein structure: the significance of the root-mean-square deviation. Journal of molecular biology 138, 321-333.
Coutsias, E.A., Seok, C., Dill, K.A., 2004. Using quaternions to calculate RMSD. Journal of computational chemistry 25, 1849-1857.
Darden, T., York, D., Pedersen, L., 1993. Particle mesh Ewald: An N· log (N) method for Ewald sums in large systems. The Journal of chemical physics 98, 10089-10092.
Falnes, P.Ø., Olsnes, S., 1995. Cell-mediated reduction and incomplete membrane translocation of diphtheria toxin mutants with internal disulfides in the A fragment. Journal of Biological Chemistry 270, 20787-20793.
Gill, D.M., Uchida, T., Singer, R.A., 1972. Expression of diphtheria toxin genes carried by integrated and nonintegrated phage beta. Virology 50, 664-668.
Hess, B., Bekker, H., Berendsen, H.J., Fraaije, J.G., 1997. LINCS: a linear constraint solver for molecular simulations. Journal of computational chemistry 18, 1463-1472.
Hess, B., Kutzner, C., Van Der Spoel, D., Lindahl, E., 2008. GROMACS 4: algorithms for highly efficient, load-balanced, and scalable molecular simulation. Journal of chemical theory and computation 4, 435-447.
Honig, B., Ray, A., Levinthal, C., 1976. Conformational flexibility and protein folding: rigid structural fragments connected by flexible joints in subtilisin BPN. Proceedings of the National Academy of Sciences 73, 1974-1978.
Housaindokht, M.R., Monhemi, H., 2013. The open lid conformation of the lipase is explored in the compressed gas: New insights from molecular dynamic simulation. Journal of Molecular Catalysis B: Enzymatic 87, 135-138.
Kumar, A., Purohit, R., 2012. Computational centrosomics: An approach to understand the dynamic behaviour of centrosome. Gene 511, 125-126.
9

Lobanov, M.Y., Bogatyreva, N., Galzitskaya, O., 2008. Radius of gyration as an indicator of protein structure compactness. Molecular Biology 42, 623-628.
Malito, E., Bursulaya, B., Chen, C., Surdo, P.L., Picchianti, M., Balducci, E., Biancucci, M., Brock, A., Berti, F., Bottomley, M.J., 2012. Structural basis for lack of toxicity of the diphtheria toxin mutant CRM197. Proceedings of the National Academy of Sciences 109, 5229-5234.
McLachlan, A.D., 1982. Rapid comparison of protein structures. Acta Crystallographica Section A: Crystal Physics, Diffraction, Theoretical and General Crystallography 38, 871-873.
Miyamoto, S., Kollman, P.A., 1992. SETTLE: an analytical version of the SHAKE and RATTLE algorithm for rigid water models. Journal of computational chemistry 13, 952-962.
Moskaug, J., Sandvig, K., Olsnes, S., 1988. Low pH-induced release of diphtheria toxin A-fragment in Vero cells. Biochemical evidence for transfer to the cytosol. Journal of Biological Chemistry 263, 2518-2525.
Mowshowitz, D., 2010. Readings, Problems & Answer Keys for Biology W1015, 2010: Problems & Answers. Columbia University, Biological Sciences.
Naglich, J.G., Metherall, J.E., Russell, D.W., Eidels, L., 1992. Expression cloning of a diphtheria toxin receptor: identity with a heparin-binding EGF-like growth factor precursor. Cell 69, 1051-1061.
O'Keefe, D.O., Cabiaux, V., Choe, S., Eisenberg, D., Collier, R.J., 1992. pH-dependent insertion of proteins into membranes: B-chain mutation of diphtheria toxin that inhibits membrane translocation, Glu-349----Lys. Proceedings of the National Academy of Sciences 89, 6202-6206.
Papini, E., Rappuoli, R., Murgia, M., Montecucco, C., 1993. Cell penetration of diphtheria toxin. Reduction of the interchain disulfide bridge is the rate-limiting step of translocation in the cytosol. Journal of Biological Chemistry 268, 1567-1574.
Parrinello, M., Rahman, A., Vashishta, P., 1983. Structural transitions in superionic conductors. Physical review letters 50, 1073.
Pitera, J.W., 2014. Expected distributions of root-mean-square positional deviations in proteins. The Journal of Physical Chemistry B 118, 6526-6530.
Robbins, J.B., Schneerson, R., Trollfors, B., Sato, H., Sato, Y., Rappuoli, R., Keith, J.M., 2005. The diphtheria and pertussis components of diphtheria-tetanus toxoids-pertussis vaccine should be genetically inactivated mutant toxins. Journal of Infectious Diseases 191, 81-88.
Satpathy, R., Guru, R., Behera, R., 2010. Computational QSAR analysis of some physiochemical and topological descriptors of Curcumin derivatives by using different statistical methods. J Chem Pharm Res 2, 344-350.
Tsai, C.J., Lin, S.L., Wolfson, H.J., Nussinov, R., 1997. Studies of protein-protein interfaces: A statistical analysis of the hydrophobic effect. Protein Science 6, 53-64.

Tsai, C.J., Nussinov, R., 1997. Hydrophobic folding units derived from dissimilar monomer structures and their interactions. Protein science 6, 24-42.
Uchida, T., Pappenheimer, A., Harper, A.A., 1972. Reconstitution of diphtheria toxin from two nontoxic cross-reacting mutant proteins. Science 175, 901-903.
van der Spoel, D., Lindahl, E., Hess, B., Van Buuren, A., Apol, E., Meulenhoff, P., Tieleman, D., Sijbers, A., Feenstra, K., van Drunen, R., 2008. GROMACS user manual version 3.3.
Vehlow, C., Stehr, H., Winkelmann, M., Duarte, J.M., Petzold, L., Dinse, J., Lappe, M., 2011. CMView: interactive contact map visualization and analysis. Bioinformatics 27, 1573-1574.

Table 1. Comparing secondary structure components of DT and E349K at different pH levels after 20 ns timescale simulations.

Secondary structure (%)	**DT (pH3)**	**E349K (pH 3)**	**DT (pH7)**	**E349K (pH7)**	**DT (pH10)**	**E349K (pH10)**
Helix	26.7	28.5	28.8	30.6	28.5	29.2
β-sheet	28.8	28.5	29.9	27.3	28.8	25.4
Turn	13.8	13.5	12.3	8.1	10.8	12.3
Coil	26.2	26.5	26.6	31.3	27.1	29.6

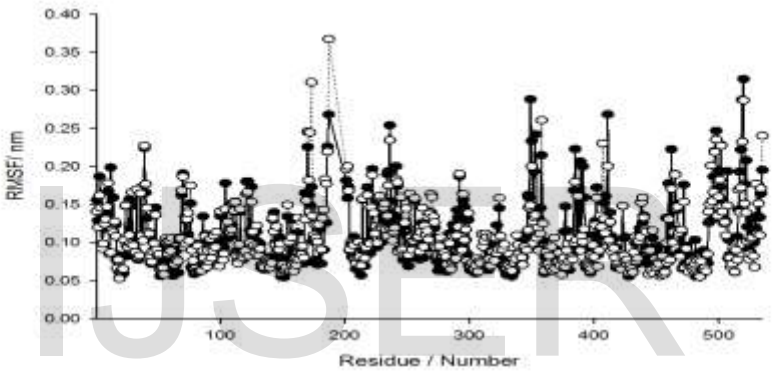

Figure. 1(A). Comparing RMSF of DT and E349K after 20 ns timescale simulation, at pH 3, the solid line and the dotted line showed E349K and DT of RMSF values respectively;

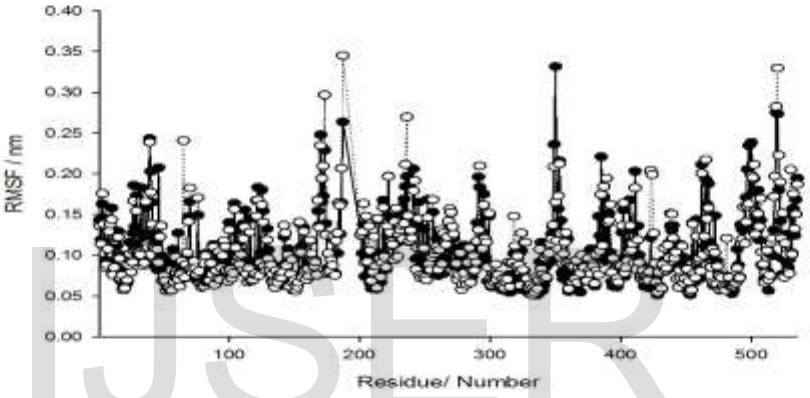

Figure. 1(B). Comparing RMSF of DT and E349K after 20 ns timescale simulation, at pH 10, the solid line and the dotted line showed E349K and DT of RMSF values respectively;

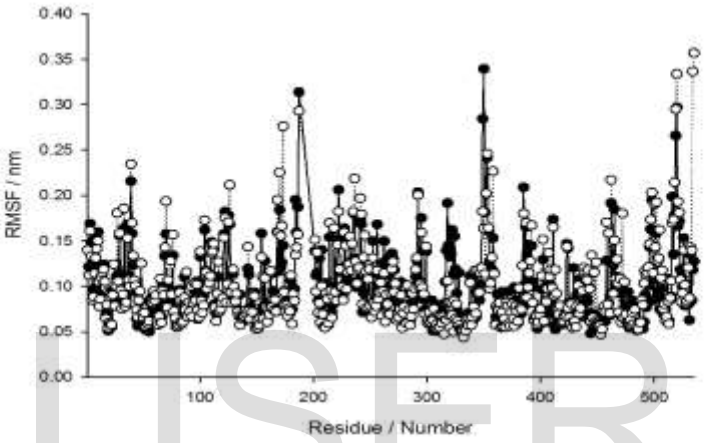

Figure. 1 (C). Comparing RMSF of DT and E349K after 20 ns timescale simulation, at pH 7, the solid line and the dotted line showed E349K and DT of RMSF values respectively;

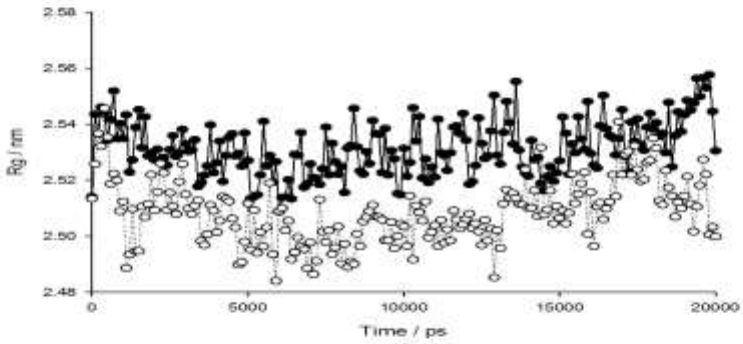

Figure. 2 (A). Comparing radius of gyration (Rg) of DT and E349K after 20 ns timescale simulation, at pH 3, the solid line and the dotted line showed E349K and DT of Rg values respectively;

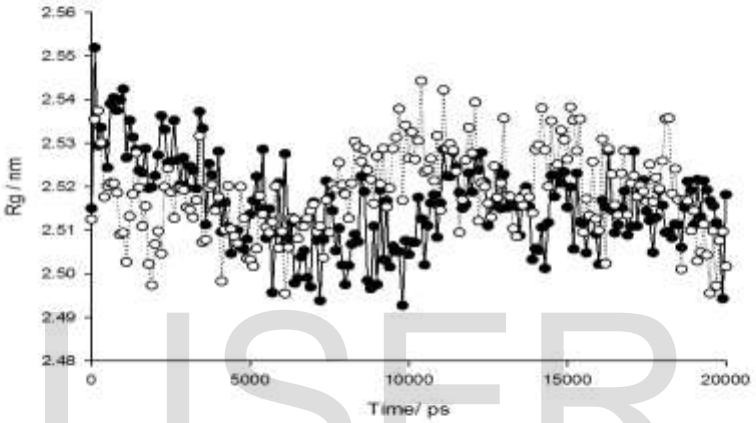

Figure. 2 (B). Comparing radius of gyration (Rg) of DT and E349K after 20 ns timescale simulation, at pH 10, the solid line and the dotted line showed E349K and DT of Rg values respectively;

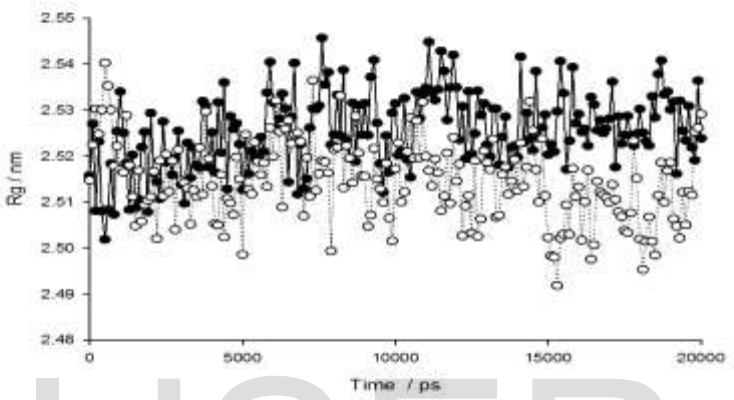

Figure. 2 (C). Comparing radius of gyration (Rg) of DT and E349K after 20 ns timescale simulation, at pH 7, the solid line and the dotted line showed E349K and DT of Rg values respectively;

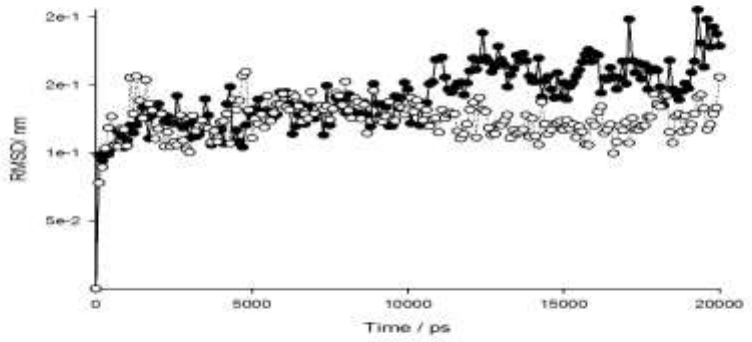

Figure. 3 (A). RMSD back bone deviation from DT and E349K after 20ns timescale simulation, at pH 3, the solid line and the dotted line showed E349K and DT of RMSD values respectively;

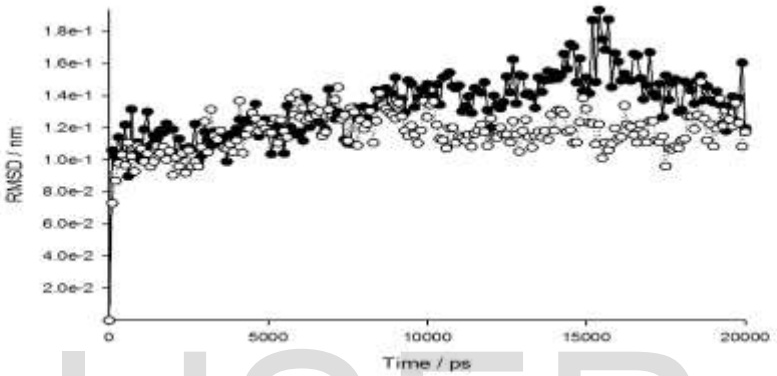

Figure. 3 (B). RMSD back bone deviation from DT and E349K after 20ns timescale simulation, at pH 10, the solid line and the dotted line showed E349K and DT of RMSD values respectively;

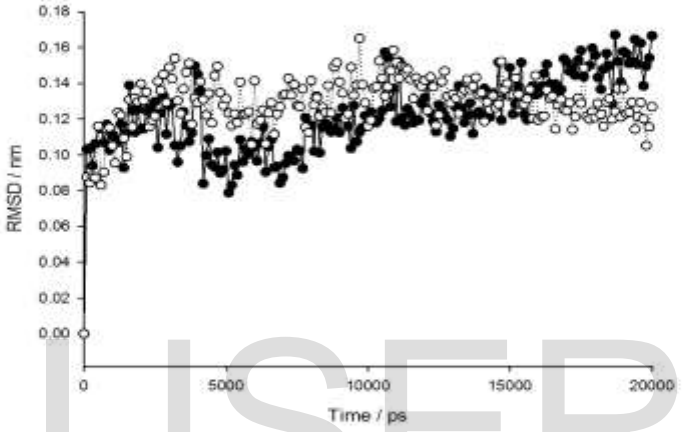

Figure. 3 (C). RMSD back bone deviation from DT and E349K after 20ns timescale simulation, at pH 7, the solid line and the dotted line showed E349K and DT of RMSD values respectively;

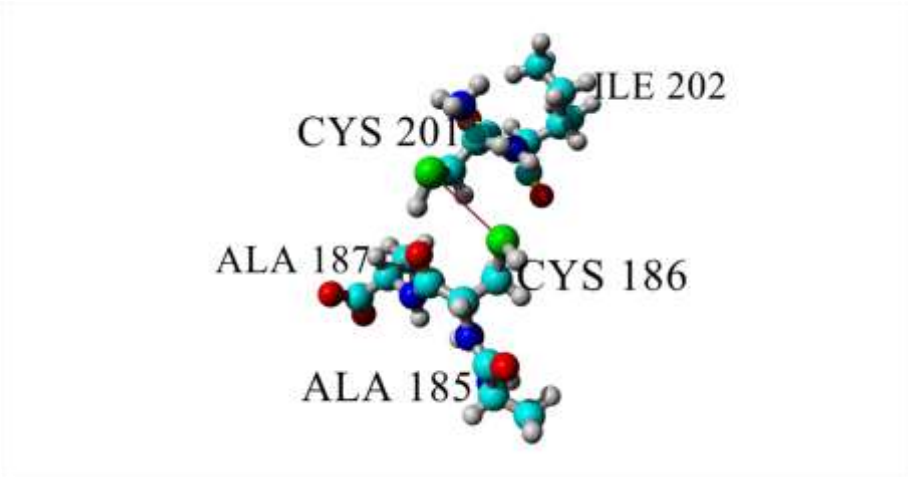

Figure.4 (A)

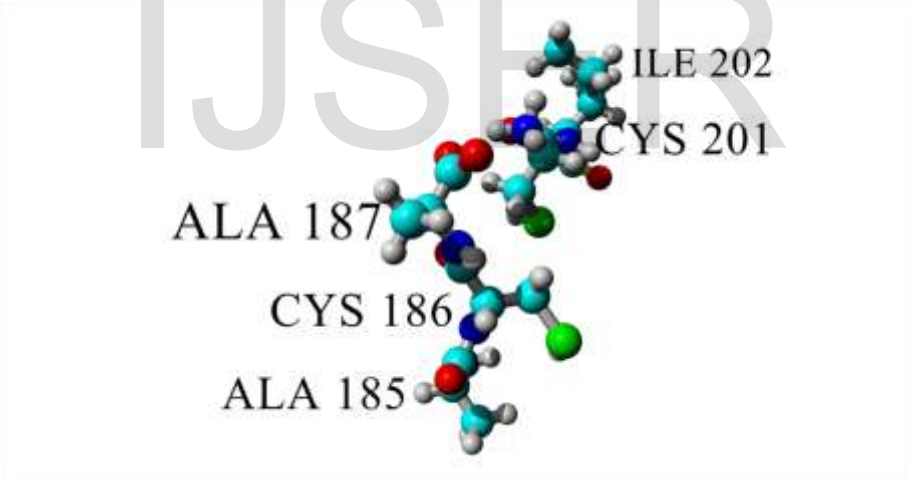

Figure. 4 (B)

Figure. 4. Snapshots of the mutant (E349K) and DT structures in the region A185-I202, after 20 ns simulation in water and at 300 K; **A:** disulfide bridge C186–C201 linked C to T domain in the DT; **B:** disulfide bridge C186–C201 linked C to T domain in the E349K